Dynamic light scattering from colloidal fractal monolayers

Pietro Cicuta* and Ian Hopkinson
Cavendish Laboratory, University of Cambridge, Madingley Road, Cambridge CB3 0HE, United Kingdom
(Received 20 December 2001; published 8 April 2002)

We address experimentally the problem of how the structure of a surface monolayer determines the viscoelasticity of the interface. Optical microscopy and surface quasielastic light scattering have been used to characterize aggregation of $CaCO_3$ particles at the air-water interface. The structures formed by cluster-cluster aggregation are two-dimensional fractals that grow to eventually form a percolating network. This process is measured through image analysis. On the same system we measure the dynamics of interfacial thermal fluctuations (surface ripplons), and we discuss how the relaxation process is affected by the growing clusters. We show that the structures start damping the ripplons strongly when the two length scales are comparable. No macroscopic surface pressure is measured and this is in contrast to lipid, surfactant, or polymer monolayers at concentrations corresponding to surface coverage. This observation and the difficulty in fitting the ripplon spectrum with traditional models suggest that a different physical mechanism might be responsible for the observed damping of ripplons in this system.

DOI: 10.1103/PhysRevE.65.041404 PACS number(s): 61.43.Hv, 68.03.−g

I. INTRODUCTION

Surface monolayers of synthetic surfactants, polymers, or biological molecules on the same lines as lipids or proteins can dramatically affect the physical properties of fluid interfaces, in particular the surface tension and the elastic and bending moduli [1]. It is also known that surface properties can be modified by the presence of small solid particles [2]. At very low surface concentrations these macromolecules are, generally, in a gas phase. Their influence on the interface properties increases dramatically when an overlap concentration is achieved. It is of interest to be able to control the interface parameters, as these in turn determine the rheology and stability of emulsions and foams, which are of technological relevance in different industries from dairy processing to oil recovery.

Cluster-cluster aggregation is an important class of growth processes. Particles aggregate into mobile clusters that further aggregate between each other to form larger clusters. In recent years a lot of work has been done to understand the kinetics of aggregation processes and the resulting structures. Well studied examples are aggregation of colloids, smoke particles, carbon black, etc. [3]. While many experiments have been performed in three dimensions, it has been simpler to perform computer simulations in two dimensions. Furthermore, many aggregation phenomena of interest, such as those occurring on a surface, are intrinsically two dimensional. For these reasons there has been an effort to perform experiments also in two dimensions. Some experiments used the air-water interface to provide a planar space, and studied first the nondiffusive aggregation of wax balls (diameter of the order of a millimeter) [4] and later the diffusion limited aggregation of silica microspheres (0.3 μm diameter) [5] on the water surface. Further experiments created a two-dimensional space through confinement between solid boundaries. For example, polystyrene spheres between glass slides (1.1 μm and 4.7 μm in diameter) were studied under various aggregating conditions [6]. While there now exists a theoretical understanding of the geometrical structures obtained from cluster-cluster aggregation, together with detailed experimental studies, there are few investigations of dynamical and rheological properties and, as far as we know, no experiments have been performed in two dimensions [7].

We were motivated to study a system where the dynamical interfacial parameters could be compared to the geometrical structural properties of the surface aggregates. A layer of colloidal particles undergoing aggregation is an ideal choice as it can easily be probed *in situ*, and such a study would complement bulk experiments undertaken with a similar motivation [8].

II. EXPERIMENT

As a model system we have studied calcium carbonate ($CaCO_3$) particles that form at the interface between air and a solution of calcium hydroxide ($Ca(OH)_2$) as this reacts with dissolved carbon dioxide. We observe the appearance of micron-sized particles, which are effectively confined to the interface. These then aggregate forming two-dimensional structures that will be shown to be fractal. This system has been described previously [9,10], and in [9] it has been shown that the kinetics of aggregation is consistent with fast cluster-cluster aggregation conditions. Our experimental conditions are similar to those of [9] but we have studied the system that is obtained from a 0.9 g/l calcium hydroxide solution. At this concentration, higher than those investigated in [9] (0.1–0.3 g/l), the cluster-cluster aggregation proceeds until a percolating network is formed after about 25 min.

The samples were prepared by mixing 20 ml of 1.2 g/l $Ca(OH)_2$ solution with 10 ml of water in a 10 cm diameter petri dish at $(23.0\pm0.1)\,^{\circ}C$ [17]. Care was taken to avoid contamination by dust, air drafts, and external vibrations during the experiments. The surface at the center of the sample was studied with two techniques. First, a time series of images of the reflected light was recorded with a 1200×1792

*Email address: pc245@cam.ac.uk

pixel digital camera (Kodak DC290) using a Zeiss Axioplan microscope, resulting in a resolution of 0.75 μm/pixel and a field of view up to 1.3 mm. Second, under the same conditions, surface dynamic light scattering (SQELS) measurements were performed, with an apparatus that is described in detail elsewhere [11]. Briefly, SQELS measures the time correlation of the intensity of light scattered by the ripplons on the liquid surface, in heterodyne conditions. Surface ripplons are the thermal fluctuations of a liquid surface, their amplitude is of the order of a few Angstroms, and their length scale ranges from the molecular to the system size. Incident light is provided by a 30-mW-He:Ne laser, illuminating a region of 5 mm diameter on the liquid surface. The spectrum of the scattered light has approximately a Lorentzian form and it can be described in terms of a frequency and a damping. It is possible in principle to analyze this spectrum in detail and determine the surface tension, the elasticity of a surface monolayer, and other surface parameters. In practice, this technique, which is described in detail in [1] and [12], has been used extensively to study interfaces of very low tensions and the surface viscoelasticity of monolayers. With our setup the accessible range of wave vectors (q) is $150 < q < 500$ cm^{-1}, corresponding to interface roughness wavelength $\lambda = 2\pi/q$ between 140 and 500 μm and frequencies (on water subphase) $15 < \omega < 100$ kHz, where $\omega = \sqrt{\gamma q^3/\rho}$, γ being the surface tension and ρ the density of the liquid subphase. The potential of this technique for investigating colloid monolayers was first shown by Earnshaw [13].

III. RESULTS

In the following we are first going to discuss the characterization of the system and then the SQELS measurements of the surface fluctuations. The digital images have been analyzed consistently throughout the time evolution using IMAGEJ and MATLAB routines. The first step was to apply a background subtraction using the ''rolling ball'' algorithm. Then the images were thresholded at a constant intensity level. These two steps provided binary images with a white background and the clusters marked as black. Figure 1 shows snapshots of the aggregating clusters on the water surface at different times. From these images we directly calculated the area fraction of black pixels and the fractal dimension D_f with the ''box counting'' algorithm [3] (box sizes 1, 2, 3, 4, 8, 12, 16, 32, and 64 were used). The clusters, clearly visible to the human eye, are composed of many closely spaced pixels. For standard cluster recognition to identify them as a connected structure, it was necessary to perform a box 7 dilation. Having labeled pixels as belonging to separate clusters, it was possible to calculate the average size, mass, number of clusters for each image. It is useful to anticipate here that while the single particles have a diameter (growing from roughly 2 μm to 10 μm), which is very small compared to the surface roughness length scales probed by SQELS, the aggregates grow to have a comparable size and eventually a single cluster spanning more than 1.3 mm is observed.

Figure 2 shows the evolution of the concentration (the fraction of black pixels) with time. There are two regimes in the concentration increase. Up to 1000 s the increase in concentration is very fast, and new $CaCO_3$ particles are formed. As they become visible in the microscope we observe their diameters to be between 1 and 3 μm. After 1000 s the increase is slower and we believe it to be due to growth of the already existing particles. This is consistent with the estimate, from the images, that the mean particle diameter is around 7 μm at 870 s and around 15 μm at 5640 s.

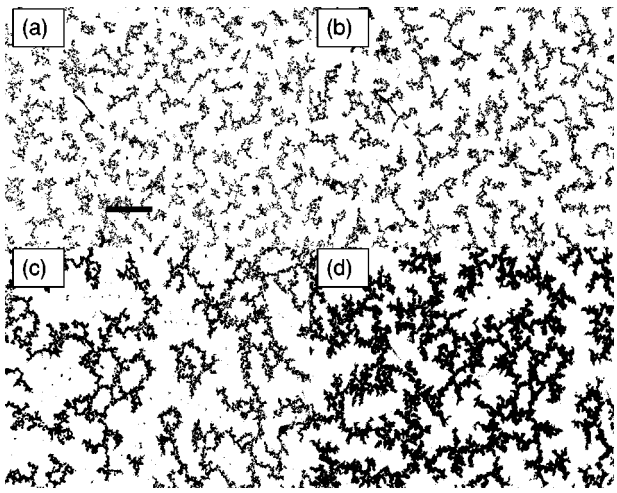

FIG. 1. Binarized optical micrographs showing the growth of fractal aggregates of $CaCO_3$ particles on a water surface. (a) 750 s, (b) 990 s, (c) 1830 s, (d) 5640 s after the creation of a clean surface. The scale bar in (a) is 200 μm; this is comparable to the surface ripplon wavelengths that are probed by SQELS.

Figure 1(a) shows the surface after 750 s, one can see that aggregation is already occurring and the surface is separated in regions of higher and lower particle concentration. Figure 1(b) shows the surface after 870 s when the presence of clusters is very clear.

Figure 3 shows the average radius of gyration $\langle R_g \rangle$ on

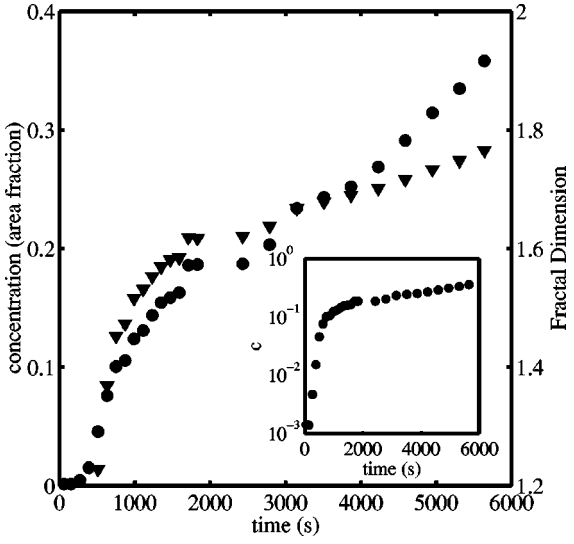

FIG. 2. Time evolution of the concentration (the fraction of black pixels in a binarized image) (●) and the fractal dimension D_f (▼) (calculated with the ''box counting'' algorithm). The inset shows the same concentration vs time data on a log-linear scale highlighting the existence of two separate regimes.

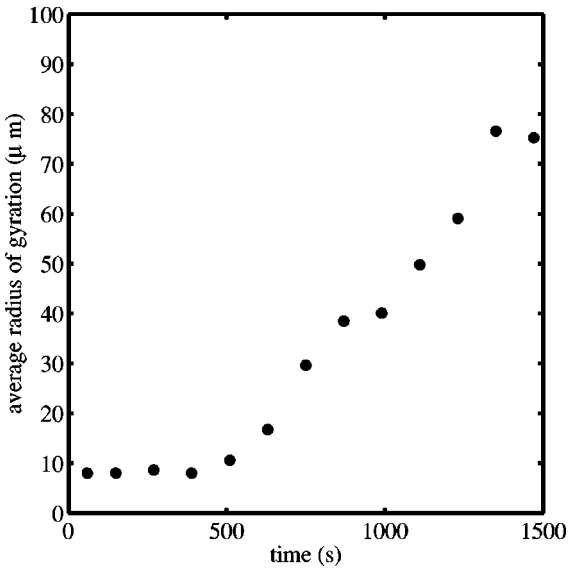

FIG. 3. Average radius of gyration. An increase in cluster size is seen from 510 s. Note that although at 990 s the $\langle R_g \rangle$ is only about 40 μm, at the same time it can be seen from Fig. 1(b) that the clusters are very elongated and extend to about 200 μm on their principal axis.

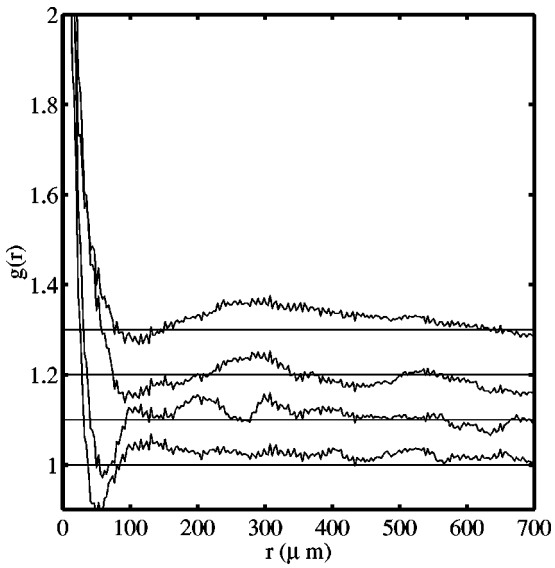

FIG. 4. Pair correlation function of black pixels. From bottom to top the times are 750 s, 990 s, 1830 s, and 5640 s, corresponding to the images in Fig. 1. The curves are shifted for comparison and the horizontal lines are at the expected asymptotic values. The minima in $g(r)$ correspond to the average cluster radius, these values are consistent with those from Fig. 3. The presence of secondary maxima indicates a loose liquid structure.

each image. The radius of gyration of the ith cluster is defined as usual as $R_{g_i} = \sqrt{(1/N)\Sigma_j (r_j - r_m)^2}$, with N the number of pixels, r_j the position of the jth pixel and r_m the position of the center of mass. The values of R_g on an image are binned into intervals and the average radius of gyration $\langle R_g \rangle$ is calculated as $\langle R_g \rangle = [\Sigma_k R_{g_k{}^2} N(k)]/[\Sigma_k R_{g_k} N(k)]$, where k identifies the bin. There is no increase in $\langle R_g \rangle$ up to 510 s, and after this it can be seen to increase roughly linearly with time. This growth cannot be followed beyond 1500 s because of the finite field of view (1.3 mm). From 1470 s onwards we observe a structure spanning more than 0.9 mm, see Fig. 1(c), while from 3150 s onwards we observe that the image is almost entirely composed of a single cluster, such as in Fig. 1(d).

Figure 4 shows the pair correlation function $g(r)$ at different times. Clearly, as aggregation proceeds, the position of the minimum in $g(r)$ shifts to bigger r and becomes shallower. A minimum in $g(r)$ is an anticorrelation, indicating that on average across the images the clusters have a certain size. The maximum in $g(r)$ occurs at the average distance between clusters. This long-ranged correlated structure appears similar to that observed on colloidal particles undergoing 3D cluster aggregation [14] and to the surface aggregation described by Earnshaw in a 2D colloidal system [15].

In Fig. 2 we show the evolution with time of the fractal dimension D_f. This has been calculated starting from 510 s, when the clusters are first present and no deviation from the expected scaling in the ''box counting'' method was observed. D_f is seen to evolve rapidly from a value of 1.23 to around 1.6 at 1500 s and to increase slowly thereafter as the structures restructure. Restructuring is observed in the form of free branches pivoting until they are doubly connected to the main cluster. This was also observed by [9] and is the probable cause for the fractal dimension being higher than that predicted for simple cluster-cluster aggregation [3].

The time correlation functions $G(\tau)$ obtained with SQELS can be fitted with the form

$$G(\tau) = B + A\cos(\omega\tau + \phi)\exp(-\Gamma\tau)\exp(-\beta^2\tau^2/4). \tag{1}$$

The final Gaussian term is the instrumental broadening, which is calibrated separately on a clean liquid surface, and ϕ is a phase term that accounts for the deviation of the power spectrum from a Lorentzian form [12]. Fitting the data with Eq. (1) yields the ripplon frequency ω and damping time Γ^{-1} [1]. These parameters describe the interface dynamics phenomenologically. No knowledge of the nature of the interface is required for this analysis, and the fitting procedure is very stable. This is in fact the only meaningful analysis of the ripplon spectrum that is possible if one does not have a model that provides a dispersion equation to relate the ripplon spectrum to the microscopic surface moduli [16]. We have measured the time evolution of ω and Γ at three different scattering angles $q = 155$, 223, and 355 cm^{-1}, respectively, corresponding to ripplon wavelengths $\lambda = 405$, 282, and 177 μm and frequencies $\omega = 14.4$, 26.8, and 53.9 kHz. For each wave vector we have repeated the experiment three times. In Figs. 5 and 6 we present the values of ω and Γ vs time, divided by their values on a clean water surface, averaged over the independent evolutions and binned in appropriate time intervals. The values of the frequency ω for $q = 155$ and 223 cm^{-1} do not vary significantly from those of the clean water surface. For $q = 355$ cm^{-1} there is, after 1200 s, a decrease of about 6%. The damping Γ retains its clean surface value up to 1000 s, when it begins to increase dramatically for all the wave vectors considered. Up to 1500 s it

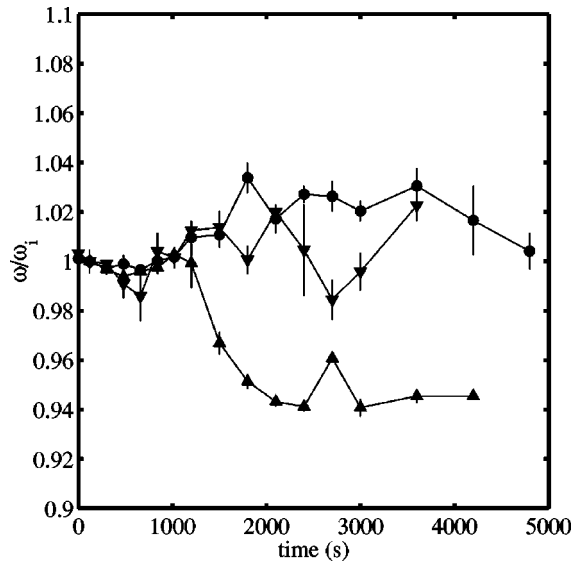

FIG. 5. Ripplon frequencies ω, normalized by their values on a clean interface ω_i, as a function of time. (▼) corresponds to a scattering vector $q=(154.5\pm0.2)$ cm^{-1}, and $\omega_i=(14.4\pm0.1)$ kHz; (●) is $q=(222.6\pm0.5)$ cm^{-1}, and $\omega_i=(26.8\pm0.2)$ kHz; (▲) is $q=(355\pm1)$ cm^{-1}, and $\omega_i=(53.9\pm0.4)$ kHz.

can be seen that the increase in damping is bigger for bigger wave vector. For $q=355$ cm^{-1} Γ has a peak at about 1500 s. As noted above, it is not possible from this data to determine physical parameters of the suface without further assumptions, but some conclusions are possible. It is only after 1000 s that the clusters have any effect on the ripplons. This means that it is not simply the presence of particles but their aggregation into larger structures that affects the wave dynamics.

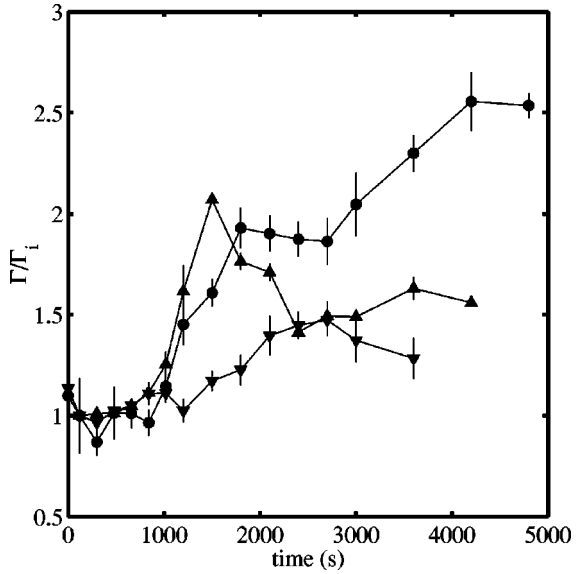

FIG. 6. Ripplon damping coefficients Γ normalized by their values on a clean interface Γ_i, as a function of time. As in Fig. 5, (▼) corresponds to a scattering vector $q=(154.5\pm0.2)$ cm^{-1}, and $\Gamma_i=(0.68\pm0.06)$ kHz; (●) is $q=(222.6\pm0.5)$ cm^{-1}, and $\Gamma_i=(0.73\pm0.03)$ kHz; (▲) is $q=(355\pm1)$ cm^{-1}, and $\Gamma_i=(2.8\pm0.1)$ kHz.

At 1000 s the diameter of the clusters calculated from the radius of gyration is about 90 μm, but the clusters already extend above the capillary wavelength scale at least in the direction of their principal axis [see Fig. 1(b)].

With the same sample preparation, the surface pressure was measured conventionally, as a function of time for up to 2 h, with a Wilhelmy filter paper plate. Starting with the clean liquid surface, no pressure increase was measured, even after the formation of the surface layer. This is in contrast to the comparable situation occurring with the absorption of surface active molecules on a surface, where the surface layer sustains a surface pressure as soon as the molecules on the surface form a percolating film.

It is important to try to determine the microscopic physical parameters that give rise to the observed ω and Γ. This is possible in many cases, as, for example, when observing the thermal ripplons on a free liquid surface or in the presence of a homogeneous viscoelastic surface monolayer. However, the monolayer in the present study is composed of fractal clusters separated by free liquid surface, and it is, thus, heterogeneous on length scales comparable to those of the ripplons. We are not aware of a model that takes this into account. It might be that as a first approximation to this condition one should simply consider the surface as being composed of two kinds of regions (type a and b), with different microscopic parameters, each region scattering light with ω_a,Γ_a and ω_b,Γ_b. In this case if ω_a and ω_b are close to each other, we would expect to observe an effective broadening of the scattered power spectrum in time (increase in Γ), as the clusters make the surface heterogeneous [as in Figs. 1(b) and (c)], followed by a narrowing (decrease in Γ) as the clusters grow to cover the whole surface evenly [Fig. 1(d)]. This qualitative behavior of Γ is indeed observed, in Fig. 6 for $q=355$ cm^{-1}, but this cannot be considered conclusive of the validity of this approximation, since a uniform layer can lead to similar behavior of Γ (see, for example, typical data from polymer monolayers [1] as a function of increasing concentration). For lack of a model that takes the heterogeneous quality of the surface into account, we have tried to describe the observed behavior following the analysis that is appropriate if a homogeneous viscoelastic monolayer is present on the surface. It is well known [1] that the dispersion relation $D(\omega)$ for waves at an air-liquid interface, bearing a thin viscoelastic layer, is given by

$$D(\omega)=[\epsilon q^2+i\omega\eta(q+m)]\left[\gamma q^2+i\omega\eta(q+m)-\frac{\rho\omega^2}{q}\right]-[i\omega\eta(m-q)]^2, \tag{2}$$

where $m=\sqrt{q^2+i(\omega\rho/\eta)}$, $\mathrm{Re}(m)>0$, η is the subphase viscosity, ρ is the subphase density, γ is the surface tension, and ϵ is the dilational modulus. Solving this equation for $D(\omega)=0$ gives an expression for the complex wave frequency ω as a function of the scattering vector q. The solutions describe both dilational and transverse waves. In a light scattering experiment it is only the transverse waves that scatter light and their power spectrum $P_q(\omega)$ is given by

$$P_q(\omega)=\frac{k_BT}{\pi\omega}\mathrm{Im}\left[\frac{i\omega\eta(m+q)+\epsilon q^2}{D(\omega)}\right]. \tag{3}$$

It is possible to fit the correlation function data with the Fourier transform of Eq. (3), yielding the values of γ, ϵ, and ϵ' directly. This approach was first introduced by Earnshaw (reviewed in [12]) and recently followed by ourselves [11]. However, in the present work we have not found the fit with three free parameters, nor a fit with the surface pressure fixed to the independently measured value, to give consistent results. This could be because the time evolution of the system does not allow for enough data to be acquired, or because of the inadequacy of Eq. (2) in describing the surface layer. We tried, in analogy to many other systems [3] where the viscosity diverges approaching gelation and an elastic modulus develops only after gelation has occurred, to fit with only ϵ' as free parameter, constraining the surface pressure to the pure liquid phase value (72.2 mN/m) and the real part of the dilational modulus to zero. This gave us a dilational viscosity ϵ' that was initially zero and increased rapidly after about 1100 s. Until the use of Eq. (2) is justified, this approach certainly cannot be considered quantitatively correct.

IV. CONCLUSIONS

We were motivated to study a two-dimensional system where the rheological properties could be related to the structure. We have been successful in characterizing the aggregation process of $CaCO_3$ particles on a surface and measuring the effect of growing clusters on surface ripplons. The data presented in Figs. 5 and 6 describe the dynamics of the surface ripplons and show that the clusters begin to modify the wave relaxation process when their size is of the order of the surface wavelength. On the basis of this data it is also clear that in the initial stages of the growth, a given cluster size has a damping effect that is stronger for bigger wave vectors, suggesting that we are probing a scale dependent gelation, where percolation on the length scale of a surface wave has an effect on that ripplon's dynamics, while the macroscopic behavior of the system is still liquidlike. These are new observations. It remains to be explained how to relate the dynamical behavior to the surface layer moduli. We have suggested what the effect of a heterogeneous surface could be and we have described the difficulties in fitting the data with the conventional surface layer model. We feel that to understand the behavior shown in Figs. 5 and 6 a model is needed to specifically take into account the fractal nature of the aggregates and the heterogeneity of the surface as a whole.

ACKNOWLEDGMENTS

We acknowledge useful discussions with Rafi Blumenfeld, Martin Buzza, and Eugene Terentjev.

[1] D. Langevin, *Light Scattering by Liquid Surfaces and Complementary Techniques* (Dekker, New York, 1992).
[2] J. Lucassen, Colloids Surf. **65**, 139 (1992).
[3] P. Meakin, *Fractals, Scaling and Growth Far From Equilibrium* (Cambridge University Press, Cambridge, United Kingdom, 1998).
[4] C. Allain and B. Jouhier, J. Phys. (France) Lett. **44**, L421 (1983).
[5] A.J. Hurd and D.W. Schaefer, Phys. Rev. Lett. **54**, 1043 (1985).
[6] A. Skjeltorp, Phys. Rev. Lett. **58**, 1444 (1987).
[7] *Fractals and Disordered Systems*, 2nd ed., edited by A. Bunde and S. Havlin (Springer-Verlag, Berlin, 1996).
[8] P.N. Segre, V. Prasad, A.B. Schofield, and D.A. Weitz, Phys. Rev. Lett. **86**, 6042 (2001).
[9] T. Nakayama, A. Nakahara, and M. Matsushita, J. Phys. Soc. Jpn. **64**, 1114 (1995).
[10] H. Wickman and J. Korley, Nature (London) **393**, 445 (1998).
[11] P. Cicuta and I. Hopkinson, J. Chem. Phys. **114**, 8659 (2001).
[12] J. Earnshaw, Appl. Opt. **36**, 7583 (1997).
[13] J. Earnshaw and D. Robinson, J. Phys.: Condens. Matter **2**, 9199 (1990).
[14] M. Carpineti and M. Giglio, Phys. Rev. Lett. **68**, 3327 (1992).
[15] D. Robinson and J. Earnshaw, Phys. Rev. Lett. **71**, 715 (1993).
[16] D.M.A. Buzza, J.L. Jones, T.C.B. McLeish, and R.W. Richards, J. Chem. Phys. **109**, 5008 (1998).
[17] To avoid the complexities reported in [10], doubly distilled and deionized water was used to prepare the $Ca(OH)_2$ solution, which was kept in a glass container and used on the same day. The $Ca(OH)_2$ was Aldrich 95+%A.C.S. reagent.